

# Hybrid Method Incorporated with Meshless Approach for Electromagnetic Wave Simulation<sup>\*)</sup>

Ayumu SAITOH, Takazumi YAMAGUCHI<sup>1)</sup>, Atsushi KAMITANI and Hiroaki NAKAMURA<sup>2,3)</sup>

*Yamagata University, Yonezawa, Yamagata 992-8510, Japan*

<sup>1)</sup>*SOKENDAI, Toki, Gifu 509-5292, Japan*

<sup>2)</sup>*National Institute for Fusion Science, Toki, Gifu 509-5292, Japan*

<sup>3)</sup>*Nagoya University, Nagoya, Aichi 464-8603, Japan*

(Received 4 December 2019 / Accepted 24 February 2020)

The hybrid method based on the collocation element-free Galerkin method and the boundary element method has been applied to the 2D steady-state scattering problem of the electromagnetic wave. In addition, the performance of the proposed method has been investigated numerically. In this study, the numerical solution of the proposed method has been obtained by using the GMRES( $m$ ) method for the complex linear system. The results of computations show that the relatively smooth distribution of electric field is obtained regardless of the boundary shape. Therefore, it is found that the proposed method can be used as one of the tools for solving the 2D steady-state scattering problems of the electromagnetic wave.

© 2020 The Japan Society of Plasma Science and Nuclear Fusion Research

Keywords: electromagnetic wave simulation, element-free Galerkin method, boundary element method, Helmholtz equation, 2D steady-state scattering problem

DOI: 10.1585/pfr.15.2401026

## 1. Introduction

As is well known, the finite-difference time-domain (FDTD) method [1] is widely used for electromagnetic wave simulations and has also yielded excellent results in the field of the nuclear fusion science [2, 3]. In the FDTD method, not only a calculation cost per time step but also a memory usage can be suppressed low. However, a target domain should be divided into a set of orthogonal meshes before executing simulations. In addition, the Courant-Friedrichs-Lewy (CFL) condition must be satisfied to ensure the numerical stability of the FDTD method. Therefore, it is difficult to apply the FDTD method to the problem in which the target domain has the complex structure. In addition, the FDTD method is an explicit method. Hence, it requires a large number of time steps until obtaining a stationary solution.

As another method for electromagnetic wave simulations, the hybrid method has been proposed. In this method, the region-type method and the boundary-type method are applied to the internal and external problems, respectively. For example, the hybrid method between the finite element method and the boundary element method is well known [4, 5]. Since the standard hybrid method is one of implicit methods, a target domain and a boundary must be divided into a set of elements before executing the simulation code. However, this operation must be executed in view of the object shape and the skin effect. Therefore, it

is time-consuming.

On the other hand, some meshless methods have been so far proposed [6–9]. The major merits of meshless methods are listed as follows: the unnecessary mesh generation and the high-order continuity of the trial functions. If the concept of meshless method were incorporated into hybrid method, the above demerit of the hybrid method might be resolved.

The purpose of the present study is to develop the hybrid method based on the collocation element-free Galerkin method (EFGM) and the boundary element method (BEM) for solving the 2D steady-state electromagnetic wave scattering problem and to investigate its performance numerically.

## 2. Numerical Method

### 2.1 2D steady-state scattering problems

For simplicity, we consider a steady-state scattering problem of electromagnetic waves from a columnar objects of an arbitrary cross section. Moreover, we assume that a TE wave enters upon the normal direction toward the axis of the column. Under the above assumptions, the 2D steady-state scattering problem is governed by the following equations:

$$-(\Delta + k^2)E_z = i\omega\mu\sigma E_z \quad \text{in } \Omega_I, \quad (1)$$

$$-(\Delta + k_0^2)E_z = 0 \quad \text{in } \Omega_E, \quad (2)$$

where  $i$ ,  $\omega$ ,  $\mu$ ,  $\sigma$  and  $E_z$  denote an imaginary unit, an angular frequency, magnetic permeability of material

author's e-mail: [saitoh@yz.yamagata-u.ac.jp](mailto:saitoh@yz.yamagata-u.ac.jp)

<sup>\*)</sup> This article is based on the presentation at the 28th International Toki Conference on Plasma and Fusion Research (ITC28).

and an electrical conductivity in the scattering object,  $z$ -component of an electric field, respectively. Moreover,  $k$  and  $k_0$  are wavenumbers in the scattering object and the free space, respectively. In addition,  $\Omega_I$  and  $\Omega_E$  denote a domain bounded by a simple closed curve  $\partial\Omega$  and an infinite domain which encloses  $\Omega_I$ , respectively. In this way, the 2D steady-state scattering problem is reduced to two Helmholtz equations which are derived from the phasor form of Maxwell's equations.

As a boundary condition, we give the following equations:

$$\llbracket E_z \rrbracket = 0, \quad \left\| \left[ \frac{1}{\mu} \frac{\partial E_z}{\partial n} \right] \right\| = 0, \quad (3)$$

where  $\mathbf{n}$  indicates an unit normal vector to the boundary  $\partial\Omega$ , respectively. Furthermore,  $\llbracket \quad \rrbracket$  means the operator which denotes a gap of operand across  $\partial\Omega$ .

In order to discretize the above problem, we must derive both the weak form of (1) and the boundary integral equation of (2). By assuming that the Dirichlet boundary condition is imposed on  $\partial\Omega$ , we can get the following weak form:

$$\forall w \text{ s.t. } w|_{\partial\Omega} = 0 : J[w, E_z] = 0. \quad (4)$$

Here,  $J[w, u]$  is the functional defined by

$$J[w, u] \equiv \iint_{\Omega_I} \nabla w \cdot \nabla u \, d^2\mathbf{x} - (k^2 - i\beta) \iint_{\Omega_I} w u \, d^2\mathbf{x},$$

where  $\beta \equiv \omega\mu\sigma$ . In addition,  $\forall w \text{ s.t. } w|_{\partial\Omega} = 0$  denotes an arbitrary function  $w(\mathbf{x})$  that fulfills  $w = 0$  on  $\partial\Omega$ .

By assuming that the Sommerfeld radiation condition, (2) is transformed to be equivalent to the boundary integral equation and, its explicit form is given by

$$c(\mathbf{y})E_z(\mathbf{y}) + \oint_{\partial\Omega} \frac{\partial w^*(\mathbf{x}, \mathbf{y})}{\partial n} E_z(\mathbf{x}) ds - \oint_{\partial\Omega} w^*(\mathbf{x}, \mathbf{y}) \frac{\partial E_z(\mathbf{x})}{\partial n} ds = E_z^1(\mathbf{y}), \quad (5)$$

where  $c(\mathbf{y})$  is the shape coefficient. Moreover,  $w^*(\mathbf{x}, \mathbf{y})$  is the fundamental solution of  $-(\Delta + k_0^2)$  and  $E_z^1(\mathbf{y})$  denotes the electric field of the incident wave at  $\mathbf{y}$ .

## 2.2 Discretization

In this section, we discretize the weak form (4), the boundary integral equation (5) and the associated boundary conditions (3). To this end, let us first place the  $N$  nodes,  $\mathbf{x}_1, \mathbf{x}_2, \dots, \mathbf{x}_N$ , in  $\Omega_I \cup \partial\Omega$  and, subsequently, the weight function  $w_i(\mathbf{x})$  is assigned to the  $i$ th node. By using the weight functions, the Moving Least Squares (MLS) shape functions  $\phi_i$ 's [5, 6] can be determined by

$$\phi_i(\mathbf{x}) = \mathbf{p}^T(\mathbf{x}) M^{-1}(\mathbf{x}) \mathbf{b}_i(\mathbf{x}),$$

where  $p(\mathbf{x})$  is a linear basis defined by  $p(\mathbf{x}) = [1 \ x \ y]$ . In addition,  $M(\mathbf{x})$  and  $\mathbf{b}_i(\mathbf{x})$  are given by

$$M(\mathbf{x}) = \sum_{i=1}^N w_i(\mathbf{x}) \mathbf{p}(\mathbf{x}_i) \mathbf{p}^T(\mathbf{x}_i),$$

$$\mathbf{b}_i(\mathbf{x}) = \sum_{i=1}^N w_i(\mathbf{x}) \mathbf{p}(\mathbf{x}_i).$$

By using the resulting MLS shape functions,  $E_z(\mathbf{x})$  and  $\partial E_z(\mathbf{x})/\partial n$  are assumed as

$$E_z(\mathbf{x}) = \sum_{i=1}^N \phi_i(\mathbf{x}) \hat{u}_i,$$

$$\frac{\partial E_z(\mathbf{x})}{\partial n} = \sum_{i=1}^N (\mathbf{n}(\mathbf{x}) \cdot \nabla \phi_i(\mathbf{x})) \hat{u}_i.$$

Next,  $M$  pieces of boundary elements,  $\Gamma_1, \Gamma_2, \dots, \Gamma_M$ , are generated by connecting two adjacent nodes on  $\partial\Omega$  with a straight line. Thereafter,  $E_z$  and  $\partial E_z/\partial n$  on the  $e$ th boundary element  $\Gamma_e$  are approximated as a linear function. In the following,  $\{\mathbf{e}_1^*, \mathbf{e}_2^*, \dots, \mathbf{e}_N^*\}$  and  $\{\mathbf{e}_1, \mathbf{e}_2, \dots, \mathbf{e}_M\}$  are the orthonormal system of the  $N$ -dimensional vector space and that of the  $M$ -dimensional vector space, respectively.

From the standard manner of the collocation EFGM [8], the weak form (4) can be discretized as

$$[A - (k^2 - i\beta)B] \hat{\mathbf{u}} + C\boldsymbol{\lambda} = \mathbf{0}. \quad (6)$$

Here,  $\hat{\mathbf{u}}$  is defined by

$$\hat{\mathbf{u}} = \sum_{i=1}^N \hat{u}_i \mathbf{e}_i^*,$$

and  $\boldsymbol{\lambda}$  is the  $M$ -dimensional unknown vector. In addition,  $A$ ,  $B$  and  $C$  are given by

$$A = \sum_{i=1}^N \sum_{j=1}^N \iint_{\Omega_I} \nabla \phi_i \cdot \nabla \phi_j \, d^2\mathbf{x} \, \mathbf{e}_i^* \mathbf{e}_j^{*T},$$

$$B = \sum_{i=1}^N \sum_{j=1}^N \iint_{\Omega_I} \phi_i \phi_j \, d^2\mathbf{x} \, \mathbf{e}_i^* \mathbf{e}_j^{*T},$$

$$C = \sum_{i=1}^N \sum_{p=1}^M \phi_i(\mathbf{x}_{\eta(p)}) \mathbf{e}_i^* \mathbf{e}_p^T,$$

where  $\eta(p)$  is the global number of the  $p$ th boundary node.

From the standard manner of the BEM, the boundary integral equation (5) is discretized. The resulting equation can be written in this form:

$$H\mathbf{u} - G\mathbf{q} = \mathbf{f}, \quad (7)$$

where  $\mathbf{u}$ ,  $\mathbf{q}$  and  $\mathbf{f}$  are given by

$$\mathbf{u} = \sum_{p=1}^M u_p \mathbf{e}_p,$$

$$\mathbf{q} = \sum_{p=1}^M q_p \mathbf{e}_p,$$

$$\mathbf{f} = \sum_{p=1}^M E_z^1(\mathbf{x}_{\eta(p)}) \mathbf{e}_p.$$

In addition,  $H$  and  $G$  are given by

$$H = \sum_{e=1}^M \sum_{p=1}^M \sum_{l=1}^2 \int_{\Gamma_e} \frac{\partial w^*(\mathbf{x}, \mathbf{x}_{\eta(p)})}{\partial n} \psi_l(\xi) ds \mathbf{e}_p \mathbf{e}_{v(e,l)}^T + \sum_{p=1}^M c(\mathbf{x}_{\eta(p)}) \mathbf{e}_p \mathbf{e}_p^T,$$

$$G = \sum_{e=1}^M \sum_{p=1}^M \sum_{l=1}^2 \int_{\Gamma_e} w^*(\mathbf{x}, \mathbf{x}_{\eta(p)}) \psi_l(\xi) ds \mathbf{e}_p \mathbf{e}_{v(e,l)}^T,$$

where  $\psi_l(\xi) \equiv [1 - (-1)^l \xi]/2$ . Moreover,  $v(e, l)$  denotes the global node number of  $l$ th local node in  $\Gamma_e$ .

Finally, let us discretize the associated boundary conditions. Note that the MLS shape function  $\phi_i(\mathbf{x})$  fulfills  $\phi_i(\mathbf{x}_j) \neq \delta_{i,j}$ , where  $\delta_{i,j}$  is the Kronecker's delta. In other words,  $E_z(\mathbf{x}_i) \neq \hat{u}_i$  is satisfied. In contrast, the linear interpolation functions,  $\psi_1(\xi)$  and  $\psi_2(\xi)$ , has the Kronecker's delta function property. Hence, (3) can be discretized as

$$C^T \hat{\mathbf{u}} = \mathbf{u}, \quad D^T \hat{\mathbf{u}} = -\mu_r \mathbf{q}, \quad (8)$$

where  $D$  is given by

$$D = \sum_{i=1}^N \sum_{p=1}^M (\mathbf{n}(\mathbf{x}_{\eta(p)}) \cdot \nabla \phi_i(\mathbf{x}_{\eta(p)})) \mathbf{e}_i^* \mathbf{e}_p^T.$$

In addition,  $\mu_r$  denote a relative permeability.

Equations (6)-(8) can be written in the following linear system:

$$\begin{bmatrix} A - (k^2 - i\beta)B & C \\ HC^T + \frac{1}{\mu_r}GD^T & O \end{bmatrix} \begin{bmatrix} \hat{\mathbf{u}} \\ \lambda \end{bmatrix} = \begin{bmatrix} \mathbf{0} \\ \mathbf{f} \end{bmatrix}. \quad (9)$$

By solving (9), we can obtain the electric field  $E_z$  in  $\Omega_1 \cup \partial\Omega$ . Note that the resulting linear system has not a diagonal-dominant coefficient matrix. Furthermore, its matrix also becomes complex and asymmetric. Therefore, we adopt the GMRES( $m$ ) method for the complex linear system as the solver of (9).

### 3. Numerical Result

In this section, we investigate the performance of the proposed method numerically. In the following numerical experiments,  $\Omega_1$  is assumed as either of the following domains:

$$\Omega_1 = \{(x, y) | x^2 + y^2 < 1/4\}, \quad (10)$$

$$\Omega_1 = (-1/2, 1/2) \times (-1/2, 1/2). \quad (11)$$

Furthermore, the incident wave is given by

$$E_z^I(x, y) = H_0^{(2)}\left(k_0 \sqrt{(x-1)^2 + y^2}\right),$$

where  $H_0^{(2)}(x)$  and  $E_0$  denote the 0th order Hankel function of the second kind and the amplitude of the incident wave,

respectively. In addition, the nodes are uniformly placed in  $\Omega_1 \cup \partial\Omega$ . The weight function is given by

$$w_i(\mathbf{x}) = \omega(|\mathbf{x} - \mathbf{x}_i|),$$

$$\omega(r) = \begin{cases} 1 - 6(r/R)^2 + 8(r/R)^3 - 3(r/R)^4 & (r \leq R) \\ 0 & (r > R), \end{cases}$$

where  $R$  indicates a support radius defined by  $R = 1.2h$ . Here,  $h$  denotes the maximum distance between one node and the nearest one. Throughout the present study, the physical parameters are fixed as follows:  $k/k_0 = 6$  and  $\mu_r = 1$ . In addition, the judgment of convergence  $\varepsilon$  in GMRES method is fixed as  $\varepsilon = 10^{-12}$ .

Let us first investigate the influence of the restart coefficient  $m$  on the convergence property of the GMRES( $m$ ) method. Figure 1 indicates the residual history of GMRES( $m$ ) method. In the following, the iteration number required for the convergence is called a convergent iteration number. We see from this figure that the convergent iteration number is diminished with an increase of the value

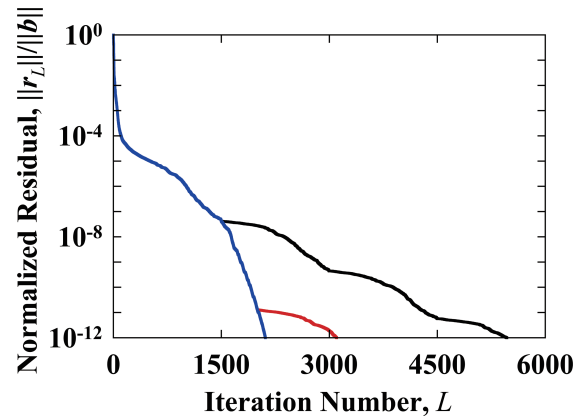


Fig. 1 Residual history of the GMRES( $m$ ) method for the case with (10) ( $N + M = 10201$ ,  $\beta = 10^4$ ). Here, the black, the red and the blue curves denote the case with  $m = 1500$ ,  $m = 2000$  and  $m = 3000$ , respectively.

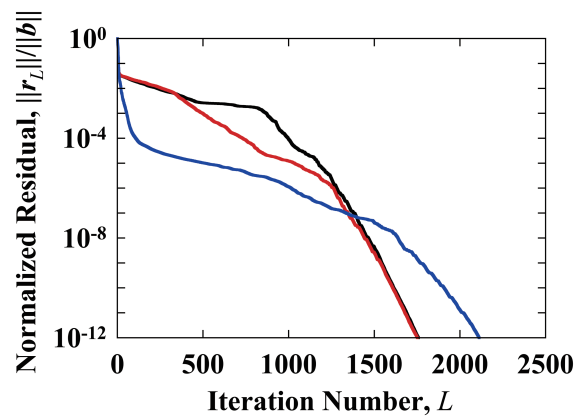


Fig. 2 Residual history of the GMRES(3000) method for the case with (10) ( $N + M = 10201$ ). Here, the black, the red and the blue curves indicate the residual histories for  $\beta = 0$ ,  $\beta = 10^2$  and  $\beta = 10^4$ , respectively.

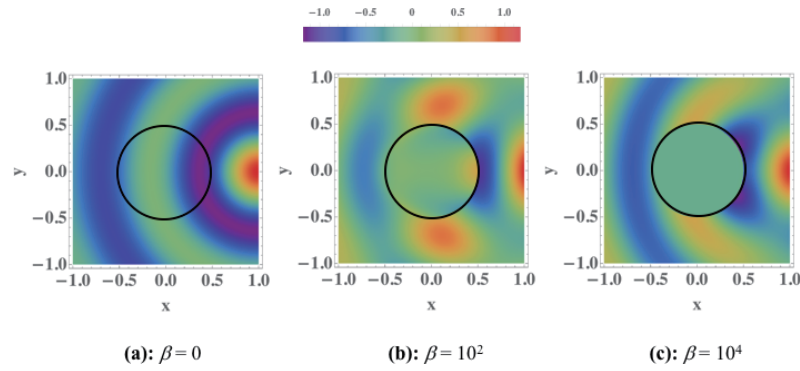


Fig. 3 The spatial distribution of  $E_z$  for the case with (10) ( $N + M = 10201$ ). Here, the black curve denotes the boundary  $\partial\Omega$ .

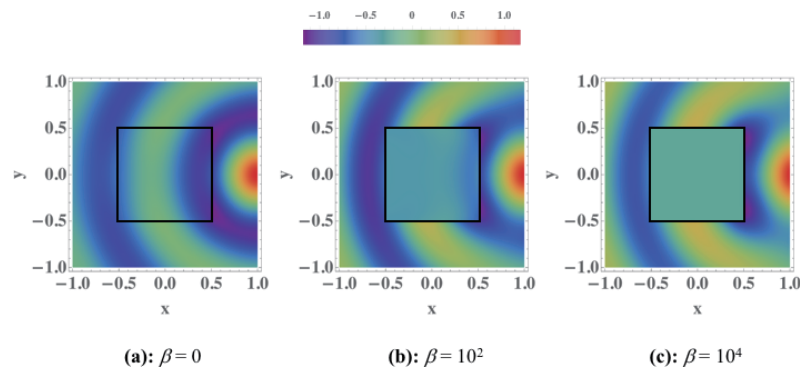


Fig. 4 The spatial distribution of  $E_z$  for the case with (11) ( $N + M = 10201$ ). Here, the black curve denotes the boundary  $\partial\Omega$ .

of  $m$ . In particular, the GMRES(3000) method is the fastest among all solvers. This result means that the convergence property of the GMRES( $m$ ) method does not improve by using the restart. However, the operation count  $P_{GM}$  and the required memory  $Q_{GM}$  of the GMRES( $m$ ) method can be estimated as follows:

$$P_{GM} = (N + M)^2 [(m + n) + (I + 1)],$$

$$Q_{GM} = (N + M)^2 + (N + M)(m + 4) + m^2/2,$$

where  $I$  and  $n$  are the total restart number and the number of an iteration after the last restart, respectively. As is apparent from the above equation,  $P_{GM}$  and  $Q_{GM}$  increase with an increase of the value of  $m$ . Hence, it is desirable to give the restart coefficient  $m$  as large as possible. Throughout the present study, the restart coefficient  $m$  is fixed as  $m = 3000$ .

On the other hand, we investigate the influence of  $\beta$  on the convergence property of the GMRES(3000) method for the case with (10). The residual history of GMRES(3000) method is shown in Fig. 2. We see from this figure that the residual norm decreases slowly with an increase in the iteration number regardless of the value of  $\beta$ . Furthermore, the convergent iteration number required for  $\beta = 10^4$  is much slower than the other two cases. This result suggests that the precondition needs to be applied to the GMRES( $m$ ) method.

Finally, we investigate the influence of the boundary shape on the accuracy of the numerical solution. The spatial distribution of the electric field for the case with (10) and (11) are shown in Figs. 3 and 4, respectively. We see from these figures that the relatively smooth distribution is obtained regardless of the value of  $\beta$ . Even if the boundary shape is changed, the distribution of  $E_z$  is gotten smoothly.

From these results, we can conclude that the proposed method can be used as one of the tools for solving the steady-state scattering problems of the electromagnetic wave.

## 4. Conclusion

We have developed the hybrid method of the BEM and the collocation EFGM for solving the 2D steady-state scattering problem of the electromagnetic wave and have investigated its performance numerically. Conclusions obtained in this paper are summarized as follows.

1. By using the proposed method, the relatively smooth distribution of the electromagnetic field is obtained regardless of the type of weight functions.
2. It is desirable to give the restart coefficient as large as possible.

For the case with the large value of  $\beta$ , the electromagnetic field cannot penetrate into the scattering object. In

this study, the node location and the number of nodes have not been changed with an increase of  $\beta$ . Therefore, the proposed hybrid method has potential for improvements of the accuracy and the speed. For future study, we will investigate the influence of the node location and the number of nodes on the performance of the proposed hybrid method. In addition, we will apply the precondition to the GMRES( $m$ ) method for improving the solver speed and also investigate the optical character of complex structure by using the developed code.

## Acknowledgment

This work was partly supported by the NIFS Collaboration Research program (NIFS18KKGS023, NIFS19KNXN379).

- [1] K. Yee, *IEEE Trans. Antennas Propag.* **14**(3), 302 (1966).
- [2] H. Nakamura, N. Kashima, A. Takayama, K. Sawada, Y. Tamura, S. Fujiwara and S. Kubo, *J. Phys. Conf. Series* **410**, 012046 (2013).
- [3] Y. Fujita, S. Ikuno, S. Kubo and H. Nakamura, *Jpn. J. Appl. Phys.* **55**, 01AH06 (2015).
- [4] Z. Xiang and Y. Lu, *Prog. Electromagnetics Res.* **22**, 107 (1999).
- [5] F. Casenave, A. Ern and G. Sylvnd, *J. Comput. Phys.* **257**(A), 627 (2014).
- [6] T. Belytchko, Y.Y. Lu and L. Gu, *Int. J. Numer. Methods Eng.* **37**, 229 (1994).
- [7] S.N. Atluri and T. Zhu, *Comput. Mech.* **22**(2), 117 (1998).
- [8] A. Kamitani, T. Takayama, T. Itoh and H. Nakamura, *Plasma Fusion Res.* **6**, 2401074 (2011).
- [9] A. Saitoh, K. Miyashita, T. Itoh, A. Kamitani, T. Isokawa, N. Kamiura and N. Matsui, *IEEE Trans. Magn.* **49**(5), 1601 (2013).